http://hdl.handle.net/2440/11163

Chiral behavior of the rho meson in lattice QCD

D. B. Leinweber, A. W. Thomas, K. Tsushima, and S. V. Wright

Department of Physics and Mathematical Physics and Special Research Centre for the Subatomic Structure of Matter,
University of Adelaide, Adelaide 5005, Australia
(Received 30 April 2001; published 8 October 2001)

In order to guide the extrapolation of the mass of the rho meson calculated in lattice QCD with dynamical fermions, we study the contributions to its self-energy, which vary most rapidly as the quark mass approaches zero, from the processes $\rho \rightarrow \omega \pi$ and $\rho \rightarrow \pi \pi$. It turns out that in analyzing the most recent data from the CP-PACS Collaboration, it is crucial to estimate the self-energy from $\rho \rightarrow \pi \pi$ using the same grid of discrete momenta as included implicitly in the lattice simulation. The correction associated with the continuum infinite volume limit can then be found by calculating the corresponding integrals exactly. Our error analysis suggests that a factor of 10 improvement in statistics at the lowest quark mass for which data currently exists would allow one to determine the physical rho mass to within 5%. Finally, our analysis throws light on a long-standing problem with the J parameter.

I. INTRODUCTION

As the lightest vector meson, the ρ is of fundamental importance in the task of deriving hadron properties from QCD. Within lattice QCD, the ratio of π to ρ masses is often used as a measure of the approach to the chiral limit. For a long time lattice calculations were restricted to values of m_π/m_ρ above 0.8. However, with the remarkable improvements in actions, algorithms, and computing power, there are now lattice QCD results with dynamical fermions available for hadron masses with current quark masses such that m_π/m_ρ is entering the chiral regime. Nevertheless, in order to compare with the properties of physical hadrons it is still necessary to extrapolate the results to realistic quark masses [1].

In the past few years there have been some very promising developments in our understanding of how to extrapolate lattice data for hadron properties, such as mass [1], magnetic moments [2], charge radii [3], and the moments of structure functions [4], to the physical region. In doing so it is vital to include the rapid variation at small pion masses associated with those pion loops, which yield the leading and next-to-leading nonanalytic behavior. (This was crucial in arriving at a reasonable value for the sigma commutator [5], for example.) However, a formal expansion of hadron properties in terms of m_π fails to converge up to the region where lattice data exist. The crucial physics insight, which renders an accurate chiral extrapolation possible, is that the source of the pion field is a complex system of quarks and gluons, with a finite size characterized by a scale Λ. When the pion mass is greater than Λ, so that the Compton wavelength of the pion is smaller than the extended source, pion loops are suppressed as powers of m_π/Λ and hadron properties are smooth slowly varying functions of the quark mass. However, for pion Compton wavelengths bigger than the source ($m_\pi < \Lambda$) one sees rapid, nonlinear variations. Phenomenologically this transition occurs at $m_\pi \sim 500$ MeV or m_π/m_ρ around 0.5—the region now being addressed by lattice simulations with dynamical fermions.

Another difficulty associated with the extrapolation of lattice results that needs further investigation is the discretization of momenta inherent in all lattice calculations. In this regard we mention not only the finite lattice spacing but the fact that there is a minimum possible nonzero momentum available because of the finite volume of the lattice. This issue is absolutely critical to the interpretation of the recent CP-PACS data for dynamical fermions [6], in which a first result[1] is reported at $m_\pi/m_\rho \sim 0.4$. As we explain in detail, the only reason that it is possible to measure the ρ mass there is that the calculation is done in a finite volume. We show that taking the finite lattice size and finite lattice spacing into account is a necessary requirement when extrapolating to the physical region. These effects become especially significant for the case of the ρ meson, which has a p-wave, two-pion decay mode.

In Sec. II we summarize the key physical ideas and the necessary formulas for extrapolating the mass of the ρ meson to the physical pion mass. This includes a discussion of the limiting behavior at small and large quark mass. We then show the result of our fitting procedure and analyze the uncertainty in extracting the ρ mass at the physical point. We show that a factor of 10 increase in the number of gauge field configurations at the lowest quark mass presently accessible would be sufficient to determine the physical ρ mass to within 5%. In Sec. III, we discuss the consequences of this analysis for the J parameter and conclude with a brief summary and outlook for the future.

II. CHIRAL EXTRAPOLATION FORMULA

The success of our earlier work concerning the extrapolation of the N and Δ masses [1] leads us to consider a similar approach to the latest two-flavor, dynamical QCD data on the ρ meson [6,7]. Once again our guiding principle is to retain those self-energy contributions which yield the most rapid

---

[1]Although CP-PACS finds no evidence of residual errors for the lowest mass point, they caution that it is premature to draw firm conclusions based on the present low statistics.
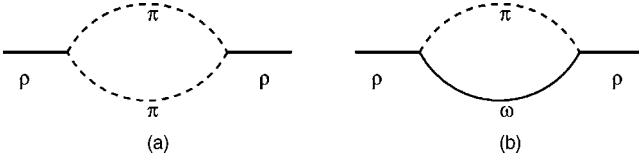
FIG. 1. The most significant self-energy contributions to the ρ meson mass.

variation with m_π near the chiral limit – i.e., those terms which yield the leading nonanalytic (LNA) behavior and the dominant next-to-leading nonanalytic (NLNA) behavior. These processes are illustrated in Fig. 1. The $\rho \to \omega \pi$ term, shown in Fig. 1(b), yields the LNA contribution to the ρ mass. The $\rho \to \pi \pi$ term [Fig. 1(a)] not only yields the NLNA behavior but, of course, the width of the ρ once m_π goes below $m_\rho/2$.

In order to evaluate these self-energy terms, we take the usual interactions [8,9]:

$$\mathcal{L}_{\rho\pi\pi} = \tfrac{1}{2} f_{\rho\pi\pi} \vec{\rho}^{\mu} \cdot [\vec{\pi} \times (\partial_\mu \vec{\pi}) - (\partial_\mu \vec{\pi}) \times \vec{\pi}] \quad (1)$$

and

$$\mathcal{L}_{\omega\rho\pi} = g_{\omega\rho\pi} \varepsilon_{\mu\nu\alpha\beta} (\partial^\mu \omega^\nu)(\partial^\alpha \vec{\rho}^\beta) \cdot \vec{\pi}. \quad (2)$$

These lead to the following expressions in the limit, where the mass of the vector mesons (ρ and ω, taken to be degenerate) is much bigger than the mass of the pion:

$$\Sigma_{\pi\pi}^{\rho} = -\frac{f_{\rho\pi\pi}^2}{6\pi^2} \int_0^\infty \frac{dk \, k^4 u_{\pi\pi}^2(k)}{w_\pi(k)(w_\pi^2(k) - \mu_\rho^2/4)}, \quad (3)$$
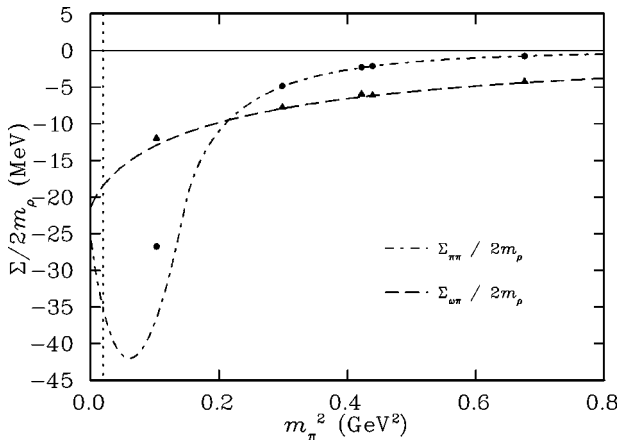

FIG. 2. Variation with pion mass of the self-energy contributions to the ρ meson, Eqs. (3) and (4), for a dipole form factor with $\Lambda_{\pi\omega} = 630$ MeV. The solid points indicate the value of the self-energy when calculated at the discrete momenta allowed on the lattices considered in this investigation. The difference between the curves and points is an indication of the physics missing because of finite lattice size and spacing.

$$\Sigma_{\pi\omega}^{\rho} = -\frac{g_{\omega\rho\pi}^2 \mu_\rho}{12\pi^2} \int_0^\infty \frac{dk \, k^4 u_{\pi\omega}^2(k)}{w_\pi^2(k)}. \quad (4)$$

In analogy with the heavy baryon limit, we have neglected the kinetic energy of the heavy vector mesons. Here $\Sigma_{\pi\omega}^{\rho}$ and $\Sigma_{\pi\pi}^{\rho}$ correspond to the processes shown in Figs. 1(a) and 1(b), respectively. The pion energy is given by $w_\pi(k) = \sqrt{k^2 + m_\pi^2}$, and $u_{\pi\pi}$ and $u_{\pi\omega}$ are dipole form factors governed by a mass parameter reflecting the finite size of the pion source. In the chiral limit these have the standard LNA and NLNA behavior (independent of the forms chosen for $u_{\pi\pi}$ and $u_{\pi\omega}$):

$$\Sigma_{\pi\pi}^{\rho}|_{\text{NLNA}} = -\frac{f_{\rho\pi\pi}^2}{4\pi^2 \mu_\rho^2} m_\pi^4 \ln(m_\pi),$$

$$\Sigma_{\pi\omega}^{\rho}|_{\text{LNA}} = -\frac{\mu_\rho g_{\omega\rho\pi}^2}{24\pi} m_\pi^3, \quad (5)$$

while they are suppressed as inverse powers of m_π once m_π is comparable with the dipole mass parameter.[2] Finally, the $\rho \to \pi\pi$ term contains the unitarity cut for $m_\pi < \mu_\rho/2$ (as well as an imaginary piece determined by the width).

The formal solution to the Dyson-Schwinger equation for the ρ propagator places the self-energy contributions in the denominator of the propagator and thereby modifies the ρ mass as [10]

$$m_\rho = \sqrt{m_0^2 + \Sigma}$$

$$\approx m_0 + \frac{\Sigma}{2m_0}, \quad (6)$$

where $\Sigma = \Sigma_{\pi\pi}^{\rho} + \Sigma_{\pi\omega}^{\rho}$ and the bare mass m_0, is taken to be analytic in the quark mass. Guided by the lattice data at large m_π, we will take m_0 to be $c_0 + c_2 m_\pi^2$.

The dipole form factors are defined as

$$u_{\pi\pi}(k) = \left(\frac{\Lambda_{\pi\pi}^2 + \mu_\rho^2}{\Lambda_{\pi\pi}^2 + 4w_\pi^2} \right)^2, \quad (7)$$

$$u_{\pi\omega}(k) = \left(\frac{\Lambda_{\pi\omega}^2 - \mu_\pi^2}{\Lambda_{\pi\omega}^2 + k^2} \right)^2, \quad (8)$$

where μ_π and μ_ρ are the physical masses of the π and ρ mesons. The normalization of $u_{\pi\pi}$ is chosen to be unity at the ρ pole and the coupling constant $f_{\rho\pi\pi} = 6.028$, is chosen to reproduce the width of the ρ (i.e., the imaginary part of the self-energy). In the $\rho \to \omega\pi$ case we take $g_{\omega\rho\pi} = 16$ GeV^{-1} [11]. The m_π^2 dependence of the self-energies of Eqs. (3) and (4) is shown in Fig. 2 by the dot-dash and dashed curves,

_____

[2]Note that all masses (e.g., the ρ mass, μ_ρ) and coupling constants should, in principle, be evaluated in the chiral limit. However, as the variations from the physical values are typically of the order 10%, we use the physical values.

respectively. The interesting behavior of the $\rho \rightarrow \pi\pi$ self-energy has been noted in many earlier works. In the context of lattice QCD, it was discussed by DeGrand [12] and by Leinweber and Cohen [10] and most recently by Szczepaniak and Swanson [13]. Other studies have looked at the self-energy as a function of p^2 (invariant mass of the vector meson) for mixed m_π [14–16].

Finally, the lattice data alone cannot separately determine $\Lambda_{\pi\pi}$ and $\Lambda_{\pi\omega}$. In order to constrain them we have therefore made the reasonable, physical assumption that the size of the source of the pion field should be the same regardless of whether the intermediate state involves an ω or a π. Thus we require that $\Lambda_{\pi\pi}$ is chosen so as to reproduce the same mean-square radius of the source as would be generated by the choice of $\Lambda_{\pi\omega}$. Equating the mean-square radii results in the following relationship:

$$\Lambda_{\pi\pi} = 2\sqrt{\Lambda_{\pi\omega}^2 - \mu_\pi^2}. \quad (9)$$

An alternative procedure, which could be imposed in future analyses, would be to constrain the difference in the meson self-energy terms to reproduce the observed $\rho - \omega$ mass difference [14–17].

Fitting procedure

As we hinted in the Introduction, the fact that CP-PACS is able to extract a measurement of the ρ mass at $m_\pi/m_\rho < 0.5$ is at first sight extremely surprising. Once the ρ is able to decay one would expect to measure not the ρ mass but the two-pion threshold. The origin of this result is the quantization of the pion momentum on the lattice and in particular the fact that the lowest (nonzero) pion momentum available is $2\pi/aL$, where is L is the spatial dimension of the lattice. For the relatively small lattice used by CP-PACS at the lowest pion mass this corresponds to more than 400 MeV/c momentum. This is why the ρ remains stable.

Motivated by Eq. (6), and wishing to preserve the correct leading nonanalytic behavior of the self-energies, we have chosen to fit the ρ mass with the simple phenomenological form:

$$m_\rho = c_0 + c_2 m_\pi^2 + \frac{\Sigma_{\pi\omega}^\rho(\Lambda_{\pi\omega}, m_\pi) + \Sigma_{\pi\pi}^\rho(\Lambda_{\pi\pi}, m_\pi)}{2(c_0 + c_2 m_\pi^2)}. \quad (10)$$

Given the constraint relating $\Lambda_{\pi\pi}$ and $\Lambda_{\omega\pi}$, this involves three adjustable parameters. At large m_π the self-energies are suppressed by inverse powers of m_π and the ρ mass becomes a simple linear function of m_π^2 (or the quark mass).

In the finite periodic volume, of the lattice, the available momenta k are discrete:

$$k_\mu = \frac{2\pi n_\mu}{aL_\mu}, \quad (11)$$

where L_μ is the number of lattice sites in the μ direction, and the integer n_μ obeys

$$-\frac{L_\mu}{2} < n_\mu \leq \frac{L_\mu}{2}. \quad (12)$$

Therefore to simulate the calculations that are done on the lattice, we should replace the continuous integrals over k in Eqs. (3) and (4) with a discrete sum over $|\vec{k}|$. However when $|\vec{k}|$ is zero, the case of a pion emitted with zero momentum, the integrands vanish, and hence do not contribute to the self-energy. In fact there is no contribution to the self-energies until $k_\mu = \pm 2\pi/aL_\mu$. There is therefore a momentum gap on the lattice for p-wave channels, produced by this discretization of momenta.

We have investigated this momentum dependence by evaluating the self-energy integrals, Eqs. (3) and (4), by summing the integrand at the allowed values of the lattice three-momenta

$$4\pi \int_0^\infty k^2\, dk = \int d^3k \approx \frac{1}{V}\left(\frac{2\pi}{a}\right)^3 \sum_{k_x, k_y, k_z},$$

where the k_μ are defined by Eqs. (11) and (12) and V is the spatial volume of the lattice. The results for the self-energy contributions are presented in Fig. 2. The self-energy calculated on the lattice (the solid circles and triangles) differs little from the full self-energy calculation in the high quark mass (m_π^2) region. Furthermore, the effect in the $\rho \rightarrow \omega\pi$ self-energy contribution is also small at low pion mass. The biggest change is in the $\rho \rightarrow \pi\pi$ self-energy calculation, at lower quark mass. This is the region in which one might expect the biggest corrections because one is approximating a principal value integral on a finite mesh. This change in behavior, particularly at the lowest data point ($m_\pi^2 \approx 0.1$ GeV^2), indicates that the $\pi\pi$ self-energy contribution is significantly understated in the lattice simulations. Upon calculating the full self-energy contribution via the continuous integrals, the magnitude of the self-energy is increased by about 10 MeV, which is 30% of the self-energy contribution at this point. These results for $\Sigma_{\pi\pi}^\rho$ and $\Sigma_{\pi\omega}^\rho$ are used in Eq. (10) to fit the lattice data.

Recent dynamical fermion lattice QCD results are presented in Fig. 3. The scale parameters relating the lattice QCD results to physical quantities have been adjusted [1] by 5% for the CP-PACS and UKQCD results. The effect is to increase the ρ mass from CP-PACS and decrease the mass from UKQCD, providing better agreement between the two independent simulations. As the χ^2 of the following fits is dominated by the CP-PACS data, we focus on this data set.

Our fits using Eq. (10) are based on the lowest five lattice masses given by CP-PACS. We selected the lowest lying masses because to move further away from the chiral limit would necessitate additional terms beyond the first two analytic terms of Eq. (10). The results of the fit are shown as the open squares in Figs. 3, 4, and 5. The parameters of the fit c_0, c_2, and $\Lambda_{\pi\omega}$, are then used in an exact evaluation of Eq. (10) using the full integrals in Eqs. (3) and (4). This result is illustrated by the solid lines in Figs. 4 and 5. We note that the value $\Lambda_{\pi\omega} = 630$ MeV for the best fit, results in a softer form factor than one might expect. We do not consider this to be
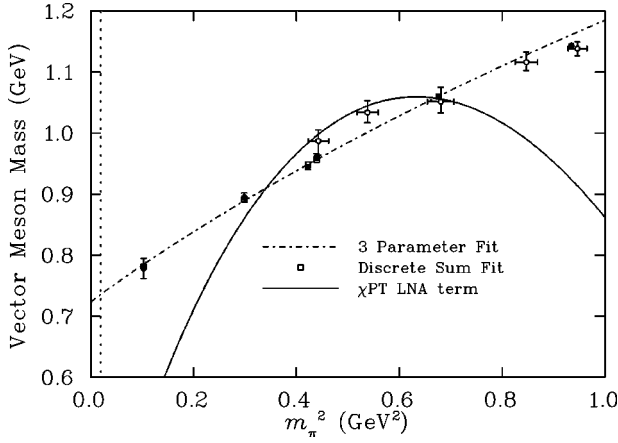
FIG. 3. Vector meson (ρ) mass from CP-PACS [6] (filled circles) and UKQCD [7] (open circles) as a function of m_π^2. The dash-dot curve is the naïve three parameter fit, Eq. (13). The open squares (which are barely distinguishable from the data) represent the fit of Eq. (10) to the data with the self-energy contributions calculated as a discrete sum of allowed lattice momenta. We have used a dipole form factor, with $\Lambda_{\pi\omega} = 630$ MeV. The solid curve is Eq. (13) with the parameter c_3 fixed to the value given by chiral perturbation theory.

of significant concern in the present paper because, as we shall discuss below, the current lattice results at low m_π are not precise enough to constrain the chiral behavior.

It is interesting to note the similarity of the results to those of Ref. [10]. There it was found that fitting quenched lattice data with a linear extrapolation, and improving the extrapolation by adding on the $\rho \to \pi\pi$ effects, predicted essentially the same physical mass, but that the chiral behavior was significantly different.

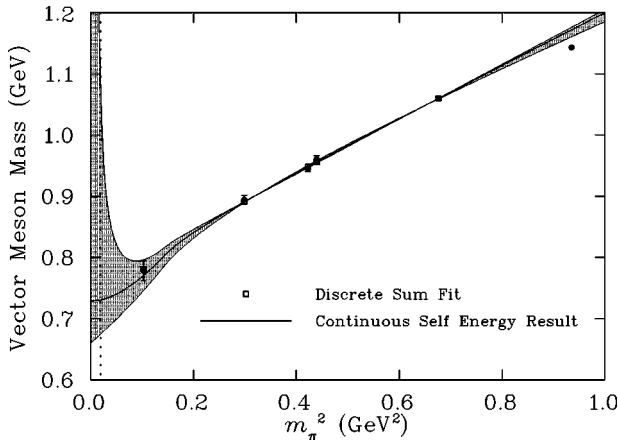FIG. 4. Analysis of the lattice data for the vector meson (ρ) mass calculated by CP-PACS as a function of m_π^2. The squares represent the fit of Eq. (10) to the data with the self-energy contributions calculated as a discrete sum of allowed lattice momenta. The solid curve is for continuous (integral) self-energy contributions to Eq. (10). We have used a dipole form factor, with optimal $\Lambda_{\pi\omega} = 630$ MeV. The shaded area is bounded below by a 1σ error bar. The upper bound is limited by the constraint $\Lambda_{\pi\omega} > \mu_\pi$, as discussed in the text.
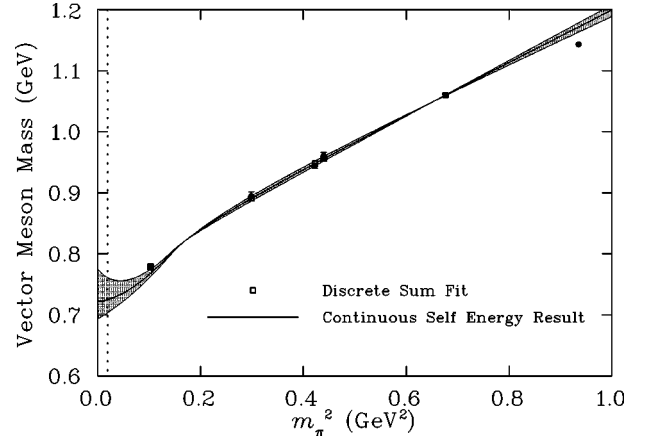
FIG. 5. The graph is as described in Fig. 3 except that the error bar on the lowest data point ($m_\pi^2 \approx 0.1$ GeV^2) has been reduced by a factor of $\sqrt{10}$. This equates to an improvement of ten times in the statistics, which we do not consider an unreasonable goal for the future. The dipole mass of the best fit is then $\Lambda_{\pi\omega} = 660$ MeV. The shaded area is bounded above and below by a 1σ error bar.

For comparison, we also show a popular three parameter fit, motivated by chiral perturbation theory:

$$m_\rho = c_0 + c_2 m_\pi^2 + c_3 m_\pi^3. \tag{13}$$

This naïve three parameter fit is illustrated by the dash-dot curve in Fig. 3. However, since the value of c_3 in Eq. (13) is commonly treated as a fitting parameter, we are not guaranteed that it has the correct value required by chiral perturbation theory (χPT). The value for the best fit is found to be -0.21 GeV^{-2}. As outlined above, our expressions for the ρ self-energies have the correct LNA and NLNA coefficients by construction. Indeed, if the coefficient c_3 is constrained to the correct value[3] ($-g_{\omega\rho\pi}^2/48\pi = -1.70$ GeV^{-2}), the best fit possible by varying c_1 and c_2 is shown as the solid line in Fig. 3. As was also found in the case of the nucleon [1], the lack of convergence of the formal expansion is such that it is not sufficient to fix the coefficient of the LNA term in a cubic fit to that predicted by χPT, as the resulting form will not fit the data.

The importance of the accuracy of the lowest mass point cannot be overstated. We stress that CP-PACS emphasized the preliminary nature of the lowest data point, because of the relatively low statistics. Nevertheless, in order to prepare for future more accurate data, we have carried out a standard error analysis including this point and the results are presented in Fig. 4. The lower bound on the shaded area was found by increasing the minimum χ^2 per degree of freedom of the fit by 1. We were unable to do this with the upper bound. The result is actually limited by the physics of the

---

[3]In Ref. [18] the m_π dependence of the LNA term to the ρ mass is given by $-(1/12\pi f^2)(\frac{2}{3}g_2^2 + g_1^2)m_\pi^3$. This would result in a value of the m_π^3 coefficient of -1.71 GeV^{-2}, in excellent agreement with the value used here.

TABLE I. Table of fit parameters c_0, c_2, c_3, $\Lambda_{\pi\omega}$, the ρ-meson mass at μ_π, the value of the J parameter, and the pion mass at which the J parameter is calculated. All values are in appropriate powers of GeV. The cubic fit refers to Eq. (13) while the dipole refers to Eq. (10) with a dipole form factor. We find that the error in the J parameter is halved if the statistics on the lowest point are increased by a factor of 10.

Fit form	c_0	c_2	c_3	$\Lambda_{\pi\omega}$	M_ρ	J	m_π^2
Cubic	0.723	0.668	-0.207	$\cdots$	0.735	0.44 (8)	0.223 (7)
Dipole	0.776	0.427 32	$\cdots$	0.630	0.731	0.45 (7)	0.225 (4)

process. In the case of a dipole form factor this means $\Lambda_{\pi\omega} > \mu_\pi$, and that is the upper limit we have shown here.

It is not unreasonable to expect an improvement in the accuracy of the calculated lattice mass values, and as a Gedanken experiment we have explored the possibility of a tenfold increase in the number of gauge configurations at the lowest pion mass. For the purposes of the simulation, we did not change the value of the data point, but simply reduced the size of the error bar by $\sqrt{10}$. As can be seen in Fig. 5, the improvement in the predictive power is dramatic. The uncertainty in the physical mass has been reduced to the 2% level. Additional improvement in the accuracy of the extrapolation would result from the availability of additional data in the low pion mass region. However, it must be noted that the provision of data around 0.2 GeV^2 and higher would probably not assist greatly in the determination of the dipole mass (Λ); it is primarily determined by points nearer the physical region. We present the parameters of these fits in Table I.

We have examined the model dependence of our paper by repeating the above fits with a monopole form factor. As can be seen in Fig. 6, the model dependence is at the level of 15 MeV at the physical pion mass with current data, and would have been at the few MeV level had the error bar been reduced by a factor of $\sqrt{10}$. This reinforces the claim in Ref. [1] that this extrapolation method is not very sensitive to the form chosen for the ultraviolet cutoff.
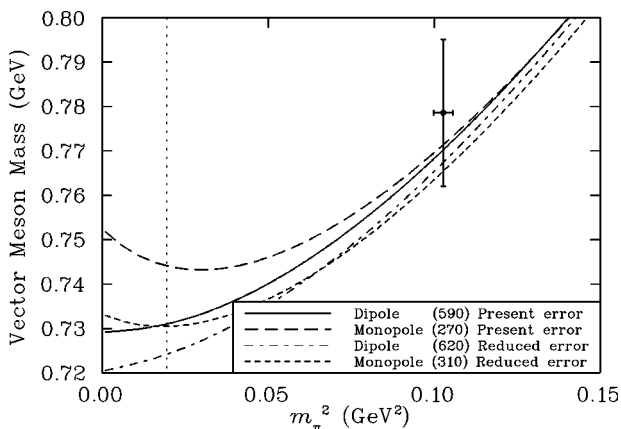

FIG. 6. A magnification of the physical pion mass region of our extrapolation results. The solid and long dashed lines represent the best fit dipole and monopole results for a fit with the present accuracy of the lattice QCD results. The dash-dot and short dashed lines are the dipole and monopole results for a reduction in the error bar of the lowest lattice data by a factor of $\sqrt{10}$. The model dependence of the choice of the form the factor is $\mathcal{O}(2\%)$.

III. J PARAMETER

A commonly perceived failure with quenched lattice QCD calculations of meson masses is the inability to correctly determine the J parameter. This dimensionless parameter was proposed as a quantitative measure, independent of chiral extrapolations, thus making it an ideal lattice observable [19]. The form of the J parameter is

$$J = m_\rho \frac{dm_\rho}{dm_\pi^2}\bigg|_{m_\rho/m_\pi=1.8} \quad (14)$$

$$\simeq m_{K*} \frac{m_{K*} - m_\rho}{m_K^2 - m_\pi^2}. \quad (15)$$

By using Eq. (15) and the experimentally measured masses of the K(495.7 MeV), K^*(892.1 MeV), π(138.0 MeV), and ρ(770.0 MeV), Lacock and Michael [19] determined

$$J = 0.48(2).$$

However, previous attempts by the lattice community to reproduce this value have been around 20% too small. In the case of quenched calculations, this has been cited as evidence of a quenching error (see, for example, the review in [20]). It was noted by Lee and Leinweber [21] that the inclusion of the self-energy of the ρ meson generated by two-pion intermediate states (excluded in the quenched calculations) acts to increase the J parameter.

In Fig. 7 we present the value of the J parameter obtained from Eq. (14) and our best fit to the lattice results using Eq. (10). The vertical dotted line indicates the value of m_π^2, where the J parameter is to be evaluated, i.e., $m_\rho/m_\pi=1.8$. The horizontal dashed line, plotted between the values of the squares of the physical pion and kaon masses, shows the experimental estimate of the J parameter from Eq. (15). This equation suggests that the evaluation of J may be approximated by the slope of the vector meson mass extrapolation between these points. The cusp shown in Fig. 7, associated with the cut in $\Sigma_{\pi\pi}^\rho$, suggests otherwise. We stress that while the detailed slope of the curve is parameter dependent, the presence of the cusp is a model independent consequence of the two pion cut in the rho spectral function.

As a point of comparison, we have also calculated J using the naïve cubic chiral extrapolation, Eq. (13), described above. The results of our investigations are summarized in Table I. The value of the J parameter is similar for both fits as it is evaluated at $m_\pi^2 \sim 0.22$ GeV^2. The effects introduced

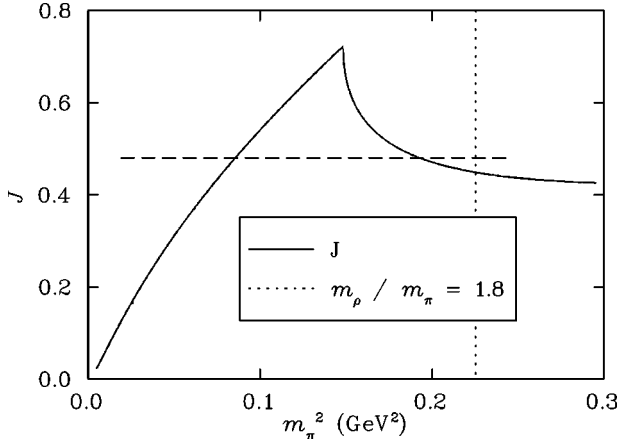FIG. 7. The solid curve is a plot of the value of the J parameter as a function of m_π^2 obtained from Eq. (14) and the best fit to the lattice results given by Eq. (10). The vertical dotted line shows the point at which the J parameter is evaluated ($m_\rho/m_\pi = 1.8$). The horizontal line displays the experimental value (0.48) plotted between the physical values of m_π^2 and m_K^2.

into the extrapolations by chiral physics do not begin playing a large role until m_π^2 falls below 0.2 GeV^2. Had the J parameter been evaluated at $m_\pi^2 = 0.19$ or 0.09 GeV^2, one would find perfect agreement with the linear ansatz of Eq. (15).

IV. CONCLUSION

We have explored the quark mass dependence of the ρ meson including the constraints imposed by chiral symmetry. The pionic self-energy diagrams are unique in that they give rise to the leading (and next-to-leading) nonanalytic behavior and yield a rapid variation of the meson mass near the chiral limit. These are the lowest energy states with given quantum numbers that have significant couplings to the ρ meson. Other meson intermediate states are suppressed by large mass terms in the denominators of the propagators, and also by smaller couplings.

We find that the predictions of two-flavor, dynamical-fermion lattice QCD results are succinctly described by Eq. (10) with terms defined in Eqs. (3) and (4) for m_π $\leqslant 800$ MeV. We have shown that our formula gives model independent results at the 2% level for the physical mass of the ρ meson. However, firm conclusions concerning agreement between the extrapolated lattice results and experiment cannot be made until the systematic errors in the extraction of the scale of masses can be reduced below the current level of 10% and accurate measurements are made at m_π ~ 300 MeV or lower.

We have also calculated the J parameter by directly evaluating the derivative of our mass extrapolation formula. We find that the empirical estimate based on differences of meson masses misses important nonanalytic effects in the derivative of m_ρ with respect to m_π^2, as illustrated in Fig. 7.

Finally we have investigated the effects of an improvement in the statistics of the lattice data. Present lattice data are not yet sufficiently precise to independently constrain the

behavior near the chiral limit. With the best data available one finds a ρ-meson mass of 731 MeV with 1σ bounds at 675 and 1062 MeV. One could constrain the bounds by using phenomenological guidance for the form factors, but we would prefer to wait for better lattice data. Figure 5 suggests that the ρ-meson mass could be known to within 5% in the very near future.

Note added. Since the submission of this manuscript, the CP-PACS Collaboration has released a preprint [22], with work showing J as a function of mass. We note that their analysis does not address the chiral physics studied here. As a result, their curves will omit the general feature of a cusp in the J parameter as discussed in this manuscript. A similar comment applies to the MILC Collaboration [23]. We look forward to seeing a similar analysis to that presented here applied to these new simulation results.

APPENDIX

In this Appendix we present the evaluation of the leading nonanalytic terms of the $\Sigma_{\pi\omega}^\rho$ and $\Sigma_{\pi\pi}^\rho$ self-energy contributions to the ρ-meson mass. By the definition in Eq. (10) all the nonanalytic behavior is contained in these two terms.

We note that the form of the self-energy contribution from $\rho \to \pi\omega$ is the same as that for the process σ_{NN} discussed in Ref. [1]. Using the results found in that paper we can write (for the choice of a sharp cutoff $[\theta(\Lambda - k)]$ for the form factor $u_{\pi\omega}$)

$$\Sigma_{\pi\omega}^\rho = -\frac{g_{\omega\rho\pi}\mu_\rho}{12\pi^2}\left[m_\pi^3\arctan\left(\frac{\Lambda}{m_\pi}\right) + \frac{\Lambda^3}{3} - \Lambda m_\pi^2\right].$$

(A1)

The chiral behavior of this expression is obtained by expanding it in m_π about $m_\pi = 0$ (the chiral limit). We find that in this limit

$$\Sigma_{\pi\omega}^\rho = -\frac{g_{\omega\rho\pi}\mu_\rho}{12\pi^2}\left(\frac{\Lambda^3}{3} - \Lambda m_\pi^2 + \frac{\pi}{2}m_\pi^3 - \frac{1}{\Lambda}m_\pi^4 + \mathcal{O}(m_\pi^6)\right),$$

(A2)

with the leading non-analytic term being of order m_π^3:

$$\Sigma_{\pi\omega}^\rho|_{\mathrm{LNA}} = -\frac{\mu_\rho g_{\omega\rho\pi}^2}{24\pi}m_\pi^3.$$

(A3)

The $\rho \to \pi\pi$ self-energy contribution is slightly more complicated. If we again choose a θ function for the form factor we can analytically integrate Eq. (3) giving

$$\Sigma_{\pi\pi}^{\rho} = -\frac{f_{\rho\pi\pi}^2}{6\pi^2}\frac{1}{2(\mu_\rho/2)}\left(2\sqrt{m_\pi^2-(\mu_\rho/2)^2}(m_\pi^2-(\mu_\rho/2)^2)\left\{\arctan\left(\frac{\Lambda-(\mu_\rho/2)+\sqrt{\Lambda^2+m_\pi^2}}{\sqrt{m_\pi^2-(\mu_\rho/2)^2}}\right)\right.\right.$$

$$\left.-\arctan\left(\frac{\Lambda+(\mu_\rho/2)+\sqrt{\Lambda^2+m_\pi^2}}{\sqrt{m_\pi^2-(\mu_\rho/2)^2}}\right)-\arctan\left(\frac{m-(\mu_\rho/2)}{\sqrt{m_\pi^2-(\mu_\rho/2)^2}}\right)+\arctan\left(\frac{m+(\mu_\rho/2)}{\sqrt{m_\pi^2-(\mu_\rho/2)^2}}\right)\right\}$$

$$\left.-[3m_\pi^2-2(\mu_\rho/2)^2](\mu_\rho/2)\ln\left(\frac{\sqrt{\Lambda^2+m_\pi^2}+\Lambda}{m_\pi}\right)-\Lambda(\mu_\rho/2)\sqrt{\Lambda^2+m_\pi^2}\right), \tag{A4}$$

where Λ regulates the cutoff of the integral. The region in which we are interested (the chiral limit) has $m_\pi < (\mu_\rho/2)$. Thus the arguments of the arctans are complex. We use the relationship

$$\arctan(z) = \frac{i}{2}\ln\left(\frac{1-iz}{1+iz}\right) \tag{A5}$$

to rewrite this expression in terms of logarithms with real arguments. Collecting the logarithms together results in the following expression for the $\rho \to \pi\pi$ self-energy, for $m_\pi < (\mu_\rho/2)$:

$$\Sigma_{\pi\pi}^{\rho} = -\frac{f_{\rho\pi\pi}^2}{6\pi^2}\frac{1}{2(\mu_\rho/2)}\left\{-[(\mu_\rho/2)^2-m_\pi^2]^{3/2}\right.$$

$$\times\ln\left(\frac{m_\pi^2[m_\pi^2-(\mu_\rho/2)^2]+\Lambda^2[m_\pi^2-2(\mu_\rho/2)^2]-2\Lambda(\mu_\rho/2)\sqrt{(\Lambda^2+m_\pi^2)[(\mu_\rho/2)^2-m_\pi^2]}}{m_\pi^2[\Lambda^2+m_\pi^2-(\mu_\rho/2)^2]}\right)$$

$$\left.-[3m_\pi^2-2(\mu_\rho/2)^2](\mu_\rho/2)\ln\left(\frac{\sqrt{\Lambda^2+m_\pi^2}+\Lambda}{m_\pi}\right)-\Lambda(\mu_\rho/2)\sqrt{\Lambda^2+m_\pi^2}\right\}. \tag{A6}$$

Looking at just the lowest order, nonanalytic, terms in the expansion about $m_\pi=0$, we have

$$\Sigma_{\pi\pi}^{\rho}|_{\text{LNA}} = -\frac{f_{\rho\pi\pi}^2}{6\pi^2}\frac{1}{2(\mu_\rho/2)}\left[\left(2(\mu_\rho/2)^3-3(\mu_\rho/2)m_\pi^2+\frac{3}{4}\frac{m_\pi^4}{(\mu_\rho/2)}\right)+[3m_\pi^2-2(\mu_\rho/2)^2](\mu_\rho/2)\right]\ln(m_\pi)$$

$$= -\frac{f_{\rho\pi\pi}^2}{4\pi^2\mu_\rho^2}m_\pi^4\ln(m_\pi), \tag{A7}$$

which is the result given in Eq. (5).

---

[1] D.B. Leinweber, A.W. Thomas, K. Tsushima, and S.V. Wright, Phys. Rev. D **61**, 074502 (2000).

[2] D.B. Leinweber, D.H. Lu, and A.W. Thomas, Phys. Rev. D **60**, 034014 (1999); E.J. Hackett-Jones, D.B. Leinweber, and A.W. Thomas, Phys. Lett. B **489**, 143 (2000); D.B. Leinweber and A.W. Thomas, Phys. Rev. D **62**, 074505 (2000).

[3] E.J. Hackett-Jones, D.B. Leinweber, and A.W. Thomas, Phys. Lett. B **494**, 89 (2000).

[4] W. Detmold, W. Melnitchouk, J.W. Negele, D.B. Renner, and A.W. Thomas, hep-lat/0103006.

[5] D.B. Leinweber, A.W. Thomas, and S.V. Wright, Phys. Lett. B **482**, 109 (2000).

[6] CP-PACS-Collaboration, S. Aoki *et al.*, Phys. Rev. D **60**, 114508 (1999).

[7] UKQCD Collaboration, C.R. Allton *et al.*, Phys. Rev. D **60**, 034507 (1999).

[8] P.A. Carruthers, *Introduction to Unitary Symmetry* (Interscience, New York, 1966).

[9] R.K. Bhaduri, *Models of the Nucleon: From Quarks to Soliton*, Vol. 22 of Lecture Notes and Supplements in Physics (Addison-Wesley, Redwood City, CA, 1988).

[10] D.B. Leinweber and T.D. Cohen, Phys. Rev. D **49**, 3512 (1994).

[11] M. Lublinsky, Phys. Rev. D **55**, 249 (1997).

[12] T.A. DeGrand, Phys. Rev. D **43**, 2296 (1991).

[13] A.P. Szczepaniak and E.S. Swanson, Phys. Rev. Lett. (to be published) hep-ph/0006306.

[14] M.A. Pichowsky, S. Walawalkar, and S. Capstick, Phys. Rev. D **60**, 054030 (1999).

[15] K.L. Mitchell and P.C. Tandy, Phys. Rev. C **55**, 1477 (1997).

[16] L.C.L. Hollenberg, C.D. Roberts, and B.H.J. McKellar, Phys. Rev. C **46**, 2057 (1992).

[17] P. Geiger and N. Isgur, Phys. Rev. Lett. **67**, 1066 (1991); P. Geiger and N. Isgur, Phys. Rev. D **41**, 1595 (1990); **44**, 799 (1991).

[18] E. Jenkins, A.V. Manohar, and M.B. Wise, Phys. Rev. Lett. **75**, 2272 (1995).

[19] UKQCD Collaboration, P. Lacock and C. Michael, Phys. Rev. D **52**, 5213 (1995).

[20] T. Yoshie, Nucl. Phys. (Proc. Suppl.) **63**, 3 (1998).

[21] F.X. Lee and D.B. Leinweber, Phys. Rev. D **59**, 074504 (1999).

[22] CP-PACS Collaboration, A.A. Khan *et al.*, hep-lat/0105015.

[23] C. Bernard *et al.*, Phys. Rev. D **64**, 054506 (2001).